A Large Signal Theory of Traveling Wave Amplifiers

Including the Effects of Space Charge and Finite Coupling Between the Beam and the Circuit

By PING KING TIEN

The non-linear behavior of the traveling-wave amplifier is calculated in this paper by numerically integrating the motion of the electrons in the presence of the circuit and the space charge fields. The calculation extends the earlier work by Nordsieck and the small-C theory by Tien, Walker and Wolontis, to include the space charge repulsion between the electrons and the effect of a finite coupling between the circuit and the electron beam. It however differs from Poulter's and Rowe's works in the methods of calculating the space charge and the effect of the backward wave.

The numerical work was done using 701-type I.B.M. equipment. Results of calculation covering QC from 0.1 to 0.4, b from 0.46 to 2.56 and k from 1.25 to 2.50, indicate that the saturation efficiency varies between 23 per cent and 37 per cent for C equal to 0.1 and between 33 per cent and 40 per cent for C equal to 0.15. The voltage and the phase of the circuit wave, the velocity spread of the electrons and the fundamental component of the charge-density modulation are either tabulated or presented in curves. A method of calculating the backward wave is provided and its effect fully discussed.

1. INTRODUCTION

Theoretical evaluation of the maximum efficiency attainable in a traveling-wave amplifier requires an understanding of the non-linear behavior of the device at various working conditions. The problem has been approached in many ways. Pierce,[1] and later Hess,[2] and Birdsall[3] and Caldwell[4] investigated the efficiency or the output power, using certain specific assumptions about the highly bunched electron beam. They either assume a beam in the form of short pulses of electrons, or, specify

an optimum ratio of the fundamental component of convection current to the average or d-c current. The method, although an abstract one, generally gives the right order of the magnitude. When the usual wave concept fails for a beam in which overtaking of the electrons arises, we may either overlook effects from overtaking, or, using the Boltzman's transport equation search for solutions in series form. This attack has been pursued by Parzen[5] and Kiel,[6] although their work is far from complete. The most satisfying approach to date is Nordsieck's analysis.[7] Nordsieck followed a typical set of "electrons" and calculated their velocities and positions by numerically integrating a set of equations of motion. Poulter[8] has extended Nordsieck equations to include space charge, finite C and circuit loss, although he has not perfectly taken into account the space charge and the backward wave. Recently Tien, Walker, and Wolontis[9] have published a small C theory in which "electrons" are considered in the form of uniformly charged discs and the space charge field is calculated by computing the force exerted on one disc by the others. Results extended to finite C, have been reported by Rowe,[10] and also by Tien and Walker.[11] Rowe, using a space charge expression similar to Poulter's, computed the space charge field based on the electron distribution in time instead of the distribution in space. This may lead to appreciable error in his space charge term, although its influence on the final results cannot be easily evaluated.

In the present analysis, we shall adopt the model described by Tien, Walker and Wolontis, but wish to add to it the effect of a finite beam to circuit coupling. A space charge expression is derived taking into account the fact that the a-c velocities of the electrons are no longer small compared with the average velocity. Equations are rewritten to retain terms involving C. As the backward wave becomes appreciable when C increases, a method of calculating the backward wave is provided and the effect of the backward wave is studied. Finally, results of the calculation covering useful ranges of design and operating parameters are presented and analyzed.

2. ASSUMPTIONS

To recapitulate, the major assumptions which we have made are:

1. The problem is considered to be one dimensional, in the sense that the transverse motions of the electrons are prohibited, and the current, velocity, and fields, are functions only of the distance along the tube and of the time.

2. Only the fundamental component of the current excites waves on the circuit.

3. The space charge field is computed from a model in which the helix is replaced by a conducting cylinder, and electrons are uniformly charged discs. The discs are infinitely thin, concentric with the helix and have a radius equal to the beam radius.

4. The circuit is lossfree.

These are just the assumptions of the Tien-Walker-Wolontis model. In addition, we shall assume a small signal applied at the input end of a long tube, where the beam entered unmodulated. What we are looking for are therefore the characteristics of the tube beyond the point at which the device begins to act non-linearly. Let us imagine a flow of electron discs. The motions of the discs are computed from the circuit and the space charge fields by the familiar Newton's force equation. The electrons, in turn, excite waves on the circuit according to the circuit equation[12] derived either from Brillouin's model[13] or from Pierce's equivalent circuit.[14] The force equation, the circuit equation, and the equation of conservation of charge in kinematics,[15] are the three basic equations from which the theory is derived.

3. FORWARD AND BACKWARD WAVES

In the traveling-wave amplifier, the beam excites forward and backward waves on the circuit. (We mean by "forward" wave, the wave which propagates in the direction of the electron flow, and by "backward" wave, the wave which propagates in the opposite direction.) Because of phase cancellation, the energy associated with the backward wave is small, but increases with the beam to circuit coupling. It is therefore important to compute it accurately. In the first place, the waves on the circuit must satisfy the circuit equation[12]

$$\frac{\partial^2 V(z, t)}{\partial t^2} - v_0^2 \frac{\partial^2 V(z, t)}{\partial z^2} = v_0 Z_0 \frac{\partial^2 \rho_\omega(z, t)}{\partial t^2} \tag{1}$$

Here, V is the total voltage of the waves. v_0 and Z_0 are respectively the phase velocity and the impedance of the cold circuit. z is the distance along the tube and t, the time. ρ_ω is the fundamental component of the linear charge density. V and ρ_ω are functions of z and t. The complete solution of (1) is in the form

$$V(z) = C_1 e^{-\Gamma_0 z} + C_2 e^{\Gamma_0 z}$$

$$+ e^{-\Gamma_0 z} \frac{\Gamma_0 v_0 Z_0}{2} \int_{z'}^{z} e^{\Gamma_0 z} \rho_\omega(z) \, dz$$

$$+ e^{\Gamma_0 z} \frac{\Gamma_0 v_0 Z_0}{2} \int_{z'}^{z} e^{-\Gamma_0 z} \rho_\omega(z) \, dz \tag{2}$$

where the common factor $e^{j\omega t}$ is omitted. $\Gamma_0 = j(\omega/v_0)$, $j = \sqrt{-1}$ and ω is the angular frequency. C_1 and C_2 are arbitrary constants which will be determined by the boundary conditions at the both ends of the beam. The first two terms are the solutions of the homogeneous equation (or the complementary functions) and are just the cold circuit waves. The third and the fourth terms are functions of electron charge density and are the particular solution of the equation.

Let us consider a long traveling-wave tube in which the beam starts from $z = 0$ and ends at $z = D$. The motion of electrons observed at any particular position is periodic in time, though it varies from point to point along the beam. To simplify the picture, we may divide the beam along the tube into small sections and consider each of them as a current element uniform in z and periodic in time. Each section of beam, or each current element excites on the circuit a pair of waves equal in amplitudes, one propagating toward the right (i.e., forward) and the other, toward the left. One may in fact imagine that these are trains of waves supported by the periodic motion of the electrons in that section of the beam. Obviously, a superposition of these waves excited by the whole beam gives the actual electromagnetic field distribution on the circuit. One may thus compute the forward traveling wave at z by summing all the waves at z which come from the left. Stated more specifically, the forward traveling energy at z is contributed by the waves excited by the current elements at the left of the point z. Similarly the backward traveling energy, (or the backward wave) at z is contributed by the waves excited by the current elements at the right of the point z. It follows obviously from this picture that there is no forward wave at $z = 0$ (except one corresponding to the input signal), and no backward wave at $z = D$. (This implies that the output circuit is matched.) With these boundary conditions, (1) is reduced to

$$V(z) = V_{\text{input}}\, e^{-\Gamma_0 z} + e^{-\Gamma_0 z}\, \frac{\Gamma_0 v_0 Z_0}{2} \int_0^z e^{\Gamma_0 z} \rho_\omega(z)\, dz$$
$$+ e^{\Gamma_0 z}\, \frac{\Gamma_0 v_0 Z_0}{2} \int_z^D e^{-\Gamma_0 z} \rho_\omega(z)\, dz \tag{3}$$

Equations (2) and (3) have been obtained by Poulter.[8] The first term of (3) is the wave induced by the input signal. It propagates as though the beam were not present. The second term is the voltage at z contributed by the charges between $z = 0$ and $z = z$. It is just the voltage of the forward wave described earlier. Similarly the third term which is the voltage at z contributed by the charges between $z = z$ and $z = D$ is the voltage of the backward wave at the point z. Denote F and B respec-

tively the voltages of the forward and the backward waves, we have

$$F(z) = V_{\text{input}}\, e^{-\Gamma_0 z} + e^{-\Gamma_0 z}\, \frac{\Gamma_0 v_0 Z_0}{2} \int_0^z e^{\Gamma_0 z}\, \rho_\omega(z)\, dz \tag{4}$$

$$B(z) = e^{\Gamma_0 z}\, \frac{\Gamma_0 v_0 Z_0}{2} \int_z^D e^{-\Gamma_0 z} \rho_\omega(z)\, dz \tag{5}$$

It can be shown by direct substitution that F and B satisfy respectively the differential equations

$$\frac{\partial F(z,\, t)}{\partial z} + \frac{1}{v_0}\, \frac{\partial F(z,\, t)}{\partial t} = \frac{Z_0}{2}\, \frac{\partial \rho_\omega(z,\, t)}{\partial t} \tag{6}$$

$$\frac{\partial B(z,\, t)}{\partial z} - \frac{1}{v_0}\, \frac{\partial B(z,\, t)}{\partial t} = -\frac{Z_0}{2}\, \frac{\partial \rho_\omega(z,\, t)}{\partial t} \tag{7}$$

We put (4) and (5) in the form of (6) and (7) simply because the differential equations are easier to manipulate than the integral equations. In fact, we should start the analysis from (6) and (7) if it were not for a physical picture useful to the understanding of the problem. Equations (6) and (7) have the advantage of not being restricted by the boundary conditions at $z = 0$ and D, which we have just imposed to derive (4) and (5). Actually, we can derive (6) and (7) directly from the Brillouin model[13] in the following manner. Suppose V, I and Z_0 are respectively the voltage, current and the characteristic impedance of a transmission line system in the usual sense. $(V + IZ_0)$ must then be the forward wave and $(V - IZ_0)$ must be the backward wave. If we substituted F and B in these forms into (1) of the Brillouin's paper,[13] we should obtain exactly (6) and (7).

It is obvious that the first and third terms of (2) are respectively the complementary function and the particular solution of (6), and similarly the second and the fourth terms of (2) are respectively the complementary function and the particular solution of (7). From now on, we shall overlook the complementary functions which are far from synchronism with the beam and are only useful in matching the boundary conditions. It is the particular solutions which act directly on the electron motion. With these in mind, it is convenient to put F and B in the form

$$F(z,\, t) = \frac{Z_0 I_0}{4C}\, [a_1(y) \cos \varphi - a_2(y) \sin \varphi] \tag{8}$$

$$B(z,\, t) = \frac{Z_0 I_0}{4C}\, [b_1(y) \cos \varphi - b_2(y) \sin \varphi] \tag{9}$$

where $a_1(y)$, $a_2(y)$, $b_1(y)$ and $b_2(y)$ are functions of y. y and φ are independent variables and have been used by Nordsieck to replace the variables, z and t, such as

$$y = C \frac{\omega}{u_0} z$$

$$\varphi = \omega \left(\frac{z}{v_0} - t \right)$$

Here as defined earlier, v_0 is the phase velocity of the cold circuit and u_0 the average velocity of the electrons. They are related by the parameter b defined by Pierce as

$$\frac{u_0}{v_0} = \frac{1}{(1 - bC)}$$

C is the gain parameter also defined by Pierce,

$$C^3 = \frac{Z_0 I_0}{4 V_0}$$

in which, V_0 and I_0 are respectively the beam voltage and current. Adding (6) to (7), we obtain an important relation between F and B, that is,

$$\frac{\partial F(z, t)}{\partial z} + \frac{1}{v_0} \frac{\partial F(z, t)}{\partial t} = -\frac{\partial B(z, t)}{\partial z} + \frac{1}{v_0} \frac{\partial B(z, t)}{\partial t} \qquad (10)$$

Substituting (8) and (9) into (10) and carrying out some algebraic manipulation, we obtain

$$b_1(y) = -\frac{C}{2(1 + bC)} \frac{d}{dy} [a_2(y) + b_2(y)]$$

$$b_2(y) = \frac{C}{2(1 + bC)} \frac{d}{dy} [a_1(y) + b_1(y)] \qquad (11)$$

or

$$B(z, t) = -\frac{Z_0 I_0}{4C} \frac{C}{2(1 + bC)}$$
$$\cdot \left[\frac{d(a_2(y) + b_2(y))}{dy} \cos \varphi + \frac{d(a_1(y) + b_1(y))}{dy} \sin \varphi \right] \qquad (12a)$$

For better understanding of the problem, we shall first solve (12a) approximately. Assuming for the moment that $b_1(y)$ and $b_2(y)$ are small compared with $a_1(y)$ and $a_2(y)$ and may be neglected in the right-hand

member of the equation, we obtain for the first order solution

$$B(z, t) \cong \frac{Z_0 I_0}{4C} \left(- \frac{C}{2(1 + bC)} \left[\frac{da_1(y)}{dy} \sin \varphi + \frac{da_2(y)}{dy} \cos \varphi \right] \right) \quad (12b)$$

Of course, the solution (12b) is justified only when $b_1(y)$ and $b_2(y)$ thus obtained are small compared with $a_1(y)$ and $a_2(y)$. The exact solution[16] of B obtained by successive approximation reads

$$\begin{aligned} B(z, t) = \frac{Z_0 I_0}{4C} \Bigg(& -\frac{C}{2(1 + bC)} \left[\frac{da_1(y)}{dy} \sin \varphi + \frac{da_2(y)}{dy} \cos \varphi \right] \\ & + \frac{C^2}{4(1 + bC)^2} \left[-\frac{d^2 a_1(y)}{dy^2} \cos \varphi + \frac{d^2 a_2(y)}{dy^2} \sin \varphi \right] + \cdots \Bigg) \end{aligned} \quad (12c)$$

It may be seen that the term involving

$$\frac{C^2}{4(1 + bC)^2}$$

and the higher order terms are neglected in our approximate solution. For C equal to few tenths, the difference between (12b) and (12c) only amounts to few per cent. We thus can calculate the backward wave by (12b) or (12c) from the derivatives of the forward wave. To obtain the complete solution of the backward wave, we should add to (12b) or (12c) a solution of the homogeneous equation. We shall return to this point later.

4. WORKING EQUATIONS

With this discussion of the backward wave, we are now in a position to derive the working equations on which our calculations are based. In Nordsieck's notation, each electron is identified by its initial phase. Thus, $\varphi(y, \varphi_0)$ and $C u_0 w(y, \varphi_0)$ are respectively the phase and the ac velocity of the electron which has an initial phase φ_0. It should be remembered that y is equal to

$$C \frac{\omega}{u_0} z$$

and is used by Nordsieck as an independent variable to replace the variable z. Let us consider an electron which is at z_0 when $t = 0$ and is at z (or y) when $t = t$. Its initial phase is then

$$\varphi_0 = \frac{\omega z_0}{u_0}$$

and its phase at y is

$$\varphi(y, \varphi_0) = \omega\left(\frac{z}{v_0} - t\right)$$

$$= \omega\left(\frac{z}{u_0} - t\right) + by$$

The velocity of the electron is expressed as

$$\frac{dz}{dt} = u_0[1 + Cw(y, \varphi_0)]$$

where u_0 is the average velocity of the electrons, and, $Cu_0w(y, \varphi_0)$ as mentioned earlier, is the ac velocity of the electron when it is at the position y. The electron charge density near an electron which has an initial phase φ_0 and which is now at y, can be computed by the equation of conservation of charge,[15] it is

$$\rho(y, \varphi_0) = -\frac{I_0}{u_0}\left|\frac{d\varphi_0}{d\varphi(y, \varphi_0)}\right|\frac{1}{1 + Cw(y, \varphi_0)} \tag{13}$$

One should recall here that I_0 is the dc beam current and has been defined as a positive quantity. When several electrons with different initial phases are present at y simultaneously, a summation of

$$\left|\frac{d\varphi_0}{d(y, \varphi_0)}\right|$$

of these electrons should be used in (13). From (13), the fundamental component of the electron charge density is

$$\rho_\omega(z, t) = -\frac{1}{\pi}\frac{I_0}{u_0}\left(\sin\varphi\int_0^{2\pi} d\varphi_0 \frac{\sin\varphi(y, \varphi_0)}{1 + Cw(y, \varphi_0)}\right.$$
$$\left. + \cos\varphi\int_0^{2\pi} d\varphi_0 \frac{\cos\varphi(y, \varphi_0)}{1 + Cw(y, \varphi_0)}\right) \tag{14}$$

These are important relations given by Nordsieck and should be kept in mind in connection with later work. In addition, we shall frequently use the transformation

$$\frac{d}{dt} = \frac{dz}{dt}\frac{\partial}{\partial z} = C\omega(1 + Cw(y, \varphi_0))\frac{\partial}{\partial y}$$

which is written following the motion of the electron. Let us start from the forward wave. It is computed by means of (6). After substituting (8) and (14) into (6), we obtain by equating the $\sin\varphi$ and the $\cos\varphi$

terms

$$\frac{da_1(y)}{dy} = -\frac{2}{\pi} \int_0^{2\pi} d\varphi_0 \frac{\sin \varphi(y, \varphi_0)}{1 + Cw(y, \varphi_0)} \tag{15}$$

$$\frac{da_2(y)}{dy} = -\frac{2}{\pi} \int_0^{2\pi} d\varphi_0 \frac{\cos \varphi(y, \varphi_0)}{1 + Cw(y, \varphi_0)} \tag{16}$$

Next we shall calculate the electron motion. We express the acceleration of an electron in the form

$$\frac{d^2z}{dt^2} = C\omega u_0(1 + Cw(y, \varphi_0)) \frac{dw(y, \varphi_0)}{dy}$$

and calculate the circuit field by differentiating F in (8) and B in (12c) with respect to z. One thus obtains from Newton's law

$$2[1 + Cw(y, \varphi_0)] \frac{dw(y, \varphi_0)}{dy} = (1 + bC)[a_1(y) \sin \varphi + a_2(y) \cos \varphi]$$

$$- \frac{C}{2} \left[\frac{da_1(y)}{dy} \cos \varphi - \frac{da_2(y)}{dy} \sin \varphi \right] \tag{17}$$

$$+ \frac{C^2}{4(1 + bC)} \left[\frac{d^2a_1(y)}{dy^2} \sin \varphi + \frac{d^2a_2(y)}{dy^2} \cos \varphi \right] - \frac{2e}{u_0 m \omega C^2} E_s$$

Here E_s is the space charge field, which will be discussed in detail later. Finally a relation between $w(y, \varphi_0)$ and $\varphi(y, \varphi_0)$ is obtained by means of (13)

$$\frac{d\varphi(y, \varphi_0)}{dy} - b = \frac{w(y, \varphi_0)}{1 + Cw(y, \varphi_0)} \tag{18}$$

Equations (15), (16), (17) and (18) are the four working equations which we have derived for finite C and including space charge.

Instead of writing the equations in the above form, Rowe,[10] ignoring the backward wave, derives (15) and (16) directly from the circuit equation (1). He obtains an additional term

$$\frac{C}{2} \frac{d^2a_2}{dy^2}$$

for (15) and another term

$$\frac{C}{2} \frac{d^2a_1}{dy^2}$$

for (16). It is apparent that the backward wave, though generally a small quantity, does influence the terms involving C.

5. THE SPACE CHARGE EXPRESSION

We have mentioned earlier that the space charge field is computed from the disc-model suggested by Tien, Walker and Wolontis. In their calculation, the force excited on one disc by the other is approximated by an exponential function

$$F_s = \frac{q^2}{2\pi r_0^2 \epsilon_0} e^{-[\alpha(z'-z)/r_0]}$$

Here r_0 is the radius of the disc or the beam, q is the charge carried by each disc, and ϵ_0 is the dielectric constant of the medium. The discs are supposed to be respectively at z and z'. α is a constant and is taken equal to 2.

Consider two electrons which have their initial phases φ_0 and φ_0' and which reach the position y (or z) at times t and t' respectively. The time difference,

$$t - t' = \frac{1}{\omega}\left[\omega t - \frac{\omega}{v_0}z - \left(\omega t' - \frac{\omega}{v_0}z\right)\right] = \frac{1}{\omega}[\varphi(y, \varphi_0') - \varphi(y, \varphi_0)]$$

multiplied by the velocity of the electron $u_0[1 + Cw(y, \varphi_0')]$ is obviously the distance between the two electrons at the time t. Thus

$$(z' - z)_{t=t} = \frac{1}{\omega}[\varphi(y, \varphi_0') - \varphi(y, \varphi_0)]u_0[1 + Cw(y, \varphi_0')] \quad (19a)$$

In this equation, we are actually taking the first term of the Taylor's expansion,

$$(z' - z)_{t=t} = \frac{dz(y, \varphi_0')}{dt}\bigg|_{t=t}(t - t') + \frac{1}{2}\frac{d^2z(y, \varphi_0')}{dt^2}\bigg|_{t=t}(t - t')^2 \quad (19b)$$
$$+ \cdots$$

It is clear that the electrons at y may have widely different velocities after having traveled a long distance from the input end, but changes in their velocities, in the vicinity of y and in a time-period of around 2π, are relatively small. This is why we must keep the first term of (19b) and may neglect the higher order terms. From (19a) the space charge field E_s in (17) is

$$\frac{2e}{m\omega C^2 u_0}E_s = \left(\frac{\omega_p}{\omega C}\right)^2 \int_{-\infty}^{+\infty} e^{-k|\varphi(y, \varphi_0+\phi)-\varphi(y,\varphi_0)|[1+ Cw(y,\varphi_0+\phi)]}$$
$$d\phi \ \mathrm{sgn}\ (\varphi(\varphi_0 + \varphi) - \phi(y, \varphi_0))$$

Here, e/m is the ratio of electron charge to mass, ω_p is the electron

angular plasma frequency for a beam of infinite extent, and k is

$$k = \frac{\alpha}{\frac{\omega}{u_0} r_0} = \frac{2}{\frac{\omega}{u_0} r_0} \tag{20}$$

In the small C theory, the distribution of electrons in time or in time-phase at z is approximately the same as the distribution in z (also expressed in the unit of time-phase) at the vicinity of z. This is, however, not true when C becomes finite. The difference between the time and space distributions is the difference between unity and the factor $(1 + Cw(y, \varphi_0'))$. We can show later that the error involved in considering the time phase as the space phase can easily reach 50 per cent or more, depending on the velocity spread of the electrons.

6. NUMERICAL CALCULATIONS

Although the process of carrying out numerical computations has been discussed in Nordsieck's paper, it is desirable to recapitulate here a few essential points including the new feature added. Using the working equations (15), (16), (17) and (18),

$$\frac{da_1}{dy}, \frac{da_2}{dy}, \frac{dw}{dy} \quad \text{and} \quad \frac{d\varphi}{dy}$$

are calculable from a_1, a_2, w and φ. The distance is divided into equal intervals of Δy, and the forward integrations of a_1, a_2, w and φ are performed by a central difference formula

$$a_1(y + \Delta y) = a_1(y) + \frac{da_1}{dy}\bigg|_{y+1/2\Delta y} \cdot \Delta y$$

In addition,

$$\frac{d^2 a_1}{dy^2} \quad \text{and} \quad \frac{d^2 a_2}{dy^2}$$

in (17) are computed from the second difference formula such that

$$\frac{d^2 a_1}{dy^2}\bigg|_{y=y} = \left[\frac{da_1}{dy}\bigg|_{y+1/2\Delta y} - \frac{da_1}{dy}\bigg|_{y-1/2\Delta y}\right] \div \Delta y$$

We thus calculate the behavior along the tube by forward integration made in steps of Δy, starting from $y = 0$. At $y = 0$ the initial conditions are determined from Pierce's linearized theory. Because of its complications in notation, this will be discussed in detail in Appendix I.

Numerical calculations were carried out using the 701-type I.B.M.

TABLE I

Case No.	QC	k	C	b	μ_1	μ_2	y(SAT.)	$A(y)$(SAT.)	$|\theta(y)-\mu_2 y|$ (SAT.)
1	0.1	2.5	0.05	0.455	μ_1 max. 0.795662	-0.748052	5.6	1.26	0.415
2	0.1	2.5	0.1	0.541	μ_1 max. 0.827175	-0.787624	5.2	1.24	0.482
3	0.1	2.5	0.1	1.145	$0.941\mu_1$ max. 0.778535	-1.05370	5.6	1.31	0.820
4	0.1	2.5	0.1	1.851	$0.66\mu_1$ max. 0.550736	-1.37968	7.0	1.36	1.05
5	0.1	2.5	0.2	0.720	μ_1 max. 0.900312	-0.873606	4.8	1.02	0.726
6	0.2	1.25	0.1	0.875	μ_1 max. 0.769795	-1.04078	5.9	1.22	0.570
7	0.2	1.25	0.1	1.422	$0.951\mu_1$ max. 0.724527	-1.29469	6.0	1.30	0.803
8	0.2	1.25	0.1	2.072	$0.666\mu_1$ max. 0.512528	-1.60435	7.6	1.35	1.08
9	0.2	2.5	0.05	0.765	μ_1 max. 0.731493	-0.973376	6.2	1.30	0.412
10	0.2	2.5	0.1	0.875	μ_1 max. 0.769795	-1.04078	5.8	1.22	0.490
11	0.2	2.5	0.1	1.422	$0.941\mu_1$ max. 0.724527	-1.29469	6.0	1.26	0.720
12	0.2	2.5	0.1	2.072	$0.666\mu_1$ max. 0.512528	-1.60435	7.2	1.25	0.92
13	0.2	2.5	0.1	2.401	$0.300\mu_1$ max. 0.230930	-1.76243	12.4	1.24	1.36
14	0.2	2.5	0.15	0.976	μ_1 max. 0.812900	-1.10656	5.4	1.11	0.572
15	0.2	2.5	0.15	1.549	$0.941\mu_1$ max. 0.765101	-1.37540	5.8	1.14	1.03
16	0.2	2.5	0.15	2.2311	$0.666\mu_1$ max. 0.541234	-1.70180	7.0	1.12	1.22
17	0.2	2.5	0.15	2.575	$0.300\mu_1$ max. 0.243864	-1.86844	10.8	1.04	1.34
18	0.4	2.5	0.05	1.25	μ_1 max. 0.653014	-1.36746	7.6	1.26	0.315
19	0.4	2.5	0.1	1.38	μ_1 max. 0.701470	-1.47477	6.6	1.11	0.674
20	0.4	2.5	0.1	1.874	$0.941\mu_1$ max. 0.660223	-1.71341	7.8	1.19	1.05
21	0.4	2.5	0.1	2.458	$0.666\mu_1$ max. 0.467038	-1.99840	8.6	1.09	1.25

equipment. The problem was programmed by Miss D. C. Legaus. The cases computed are listed in Table I in which μ_1 and μ_2 are respectively Pierce's x_1 and y_1, and A, $(\theta - \mu_2 y)$ and y at saturation will be discussed later. All the cases were computed with $\Delta y = 0.2$ using a model based on 24 electron discs per electronic wavelength. To estimate the error involved in the numerical work, Case (10) has been repeated for 48 electrons and Cases (10) and (19) for $\Delta y = 0.1$. The results obtained by using different numbers of electrons are almost identical and those obtained by varying the interval Δy indicate a difference in $A(y)$ less than 1 per cent for Case (10) and about 6 per cent for Case (19). As error generally increases with QC and C the cases listed in this paper are limited to $QC = 0.4$ and $C = 0.15$. For larger QC or C, a model of more electrons or a smaller interval of integration, or both should be used.

7. POWER OUTPUT AND EFFICIENCY

Define

$$A(y) = \tfrac{1}{4}\sqrt{a_1(y)^2 + a_2(y)^2}$$

$$-\theta(y) = \tan^{-1}\frac{a_2(y)}{a_1(y)} + by \tag{21}$$

We have then

$$F(z, t) = \frac{Z_0 I_0}{C} A(y) \cos\left[\frac{\omega z}{u_0} - \omega t - \theta(y)\right] \tag{22}$$

The power carried by the forward wave is therefore

$$\left(\frac{F^2}{Z_0}\right)_{\text{average}} = 2CA^2 I_0 V_0 \tag{23}$$

and the efficiency is

$$\text{Eff.} = \frac{2CA^2 I_0 V_0}{I_0 V_0} = 2CA^2 \quad \text{or} \quad \frac{\text{Eff.}}{C} = 2CA^2 \tag{24}$$

In Table I, the values of $A(y)$, $\theta(y)$ and y at the saturation level are listed for every case computed. We mean by the saturation level, the distance along the tube or the value of y at which the voltage of the forward wave or the forward traveling power reaches its first peak. The Eff./C at the saturation level is plotted in Fig. 1 versus QC, for $k = 2.5$, b for maximum small-signal gain and $C = $ small, 0.05, 0.1, 0.15 and 2. It is also plotted versus b in Fig. 2 for $QC = 0.2$, $k = 2.5$ and $C = $ small, 0.1 and 0.15, and in Fig. 3 for $QC = 0.2$, $C = 0.1$ and $k = 1.25$ and 2.50. In Fig. 2 the dotted curves indicate the values of b at which
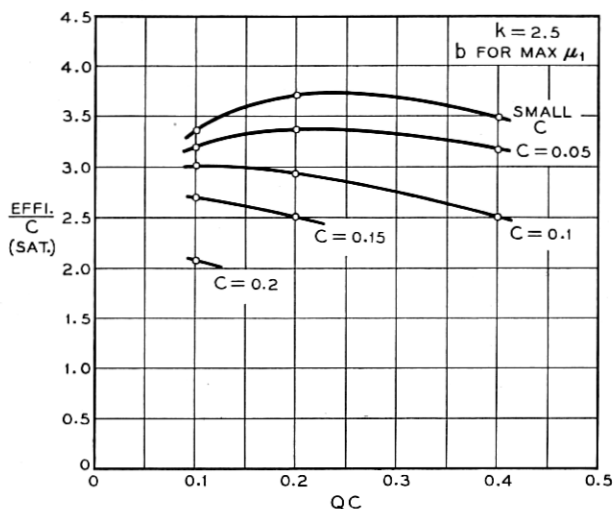
Fig. 1 — The saturation eff./C versus QC, for $k = 2.5$, b for maximum small-signal gain and C = small, 0.1, 0.15 and 0.2.

$\mu_1 = \mu_1(\text{max})$, 0.94 $\mu_1(\text{max})$, 0.67 $\mu_1(\text{max})$ and 0.3 $\mu_1(\text{max})$, respectively. It is seen that Eff./C decreases as C increases particularly when b is large. It is almost constant between $k = 1.25$ and 2.50 and decreases slowly for large values of C when QC increases.

The (Eff./C) at saturation is also plotted versus QC in Fig. 4(a) for small C, and in Fig. 4(b) for $C = 0.1$. It should be noted that for $C = 0.1$ the values of Eff./C fall inside a very narrow region say between 2.5 to 3.5, whereas for small C they vary widely.

8. VELOCITY SPREAD

In a traveling-wave amplifier, when electrons are decelerated by the circuit field, they contribute power to the circuit, and when electrons are accelerated, they gain kinetic energy at the expense of the circuit power. It is therefore of interest to plot the actual velocities of the fastest and the slowest electrons at the saturation level and find how they vary with the parameters QC, C, b and k. This is done in Fig. 5. These velocities are also plotted versus y for Case 10 in Fig. 6, in which, the $A(y)$ curve is added for reference.

9. THE BACKWARD WAVE AND THE FUNDAMENTAL COMPONENT OF THE ELECTRON CHARGE DENSITY

Our calculation of efficiency has been based on the power carried by the forward wave only. One may, however, ask about the actual power
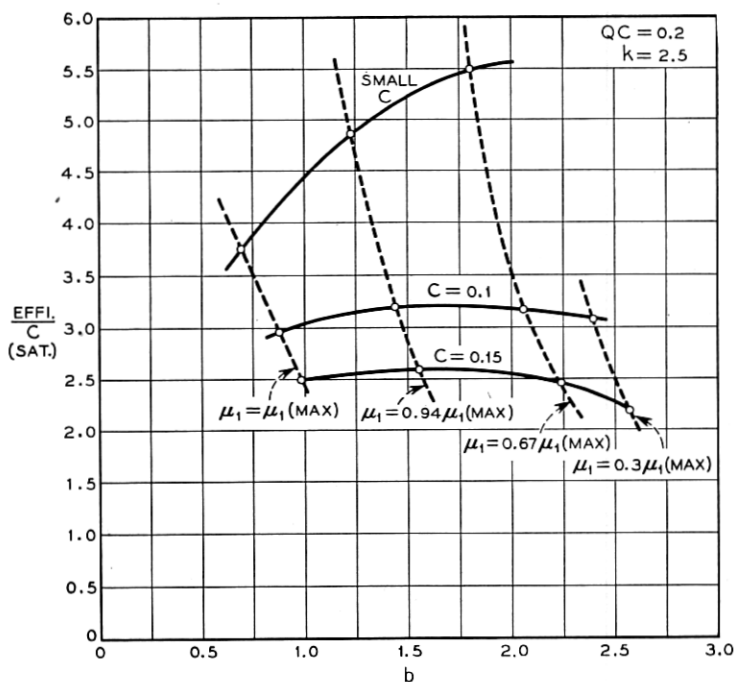
Fig. 2 — The saturation eff./C versus b, for $k = 2.5$, $QC = 0.2$, and $C =$ small, 0.1 and 0.15. The dotted curves indicate the values of b for $\mu_1 = 1, 0.94, 0.67$, and 0.3 of μ_1(max) respectively.

output in the presence of the backward wave. For simplicity, we shall use the approximate solution (12b) which can be written in the form

$B(z, t) \cong$ Real Component of

$$\left(\frac{Z_0 I_0}{4C} \frac{C}{2(1 + bC)} \sqrt{\left(\frac{da_1(y)}{dy}\right)^2 + \left(\frac{da_2(y)}{dy}\right)^2} \; e^{j\omega t - \Gamma_0 z - by + j\xi} \right) \quad (12d)$$

with

$$\tan \xi = \left(-\frac{da_1(y)}{dy} \right) \Big/ \left(-\frac{da_2(y)}{dy} \right)$$

As mentioned earlier that the complete solution of (6) is obtained by adding to (12b) a complementary function such that

$B(z, t) = C_1 e^{-j\omega t + \Gamma_0 z}$

$$+ \frac{Z_0 I_0}{4C} \frac{C}{2(1 + bC)} \sqrt{\left(\frac{da_1}{dy}\right)^2 + \left(\frac{da_2}{dy}\right)^2} \; e^{j\omega t - \Gamma_0 z - by + j\xi} \quad (25)$$
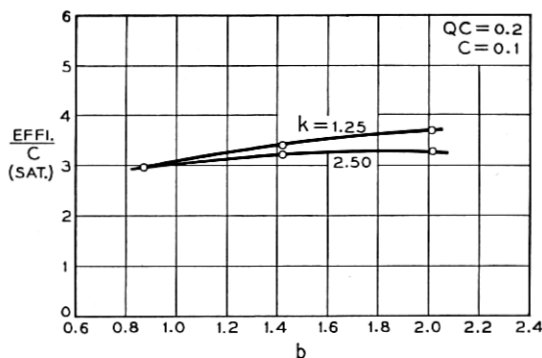
Fig. 3 — The saturation eff./C versus b, for $QC = 0.2$ $C = 0.1$ and $k = 1.25$ and 2.50.

If the output circuit is matched by cold measurements, the backward wave must be zero at the output end, $z = D$. This determines C_1, that is,

$$C_1 = -\frac{Z_0 I_0}{4C} \frac{C}{2(1 + bC)} \sqrt{\left(\frac{da_1(y)}{dy}\right)^2_{z=D} + \left(\frac{da_2(y)}{dy}\right)^2_{z=D}} e^{\Gamma_0(2+bc)D+j\xi}$$

or

$$C_1 e^{j\omega t + \Gamma_0 z} = -\frac{Z_0 I_0}{4C} \frac{C}{2(1 + bC)} \sqrt{\left(\frac{da_1(y)}{dy}\right)^2_{z=D} + \left(\frac{da_2(y)}{dy}\right)^2_{z=D}}$$
$$\cdot e^{\Gamma_0(2+bC)D+j\xi} e^{j\omega t + \Gamma_0 z} \qquad (26)$$

The backward wave therefore consists of two components. One compo-
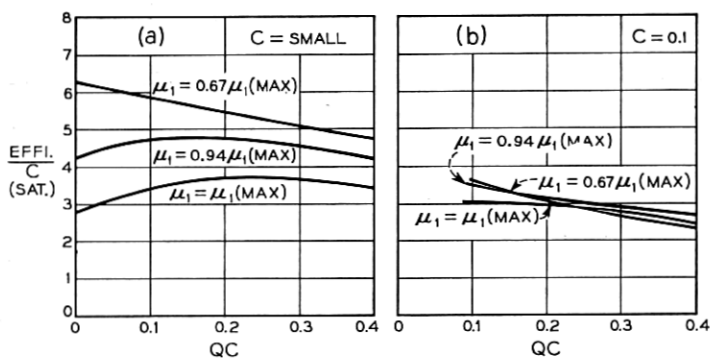
Fig. 4 — The saturation eff./C versus QC for b corresponding $\mu_1 = 1, 0.94$ and 0.67 of μ_1(max), (a) for $C =$ small, (b) for $C = 0.1$.

nent is coupled to the beam and has an amplitude equal to

$$\frac{Z_0 I_0}{4C} \frac{C}{2(1 + bC)} \sqrt{\left(\frac{da_1}{dy}\right)^2 + \left(\frac{da_2}{dy}\right)^2}$$

which generally grows with the forward wave. It thus has a much larger amplitude at the output end than at the input end. The other component is a wave of constant amplitude, which travels in the direction opposite to the electron flow with a phase velocity equal to that of the cold circuit. At the output end, $z = D$, both components have the same amplitude but are opposite in sign. One thus realizes that there exists a reflected wave of noticeable amplitude, in the form of (26), even though the output circuit is properly matched by cold measurements. Under such circumstances, the voltage at the output end is the voltage of the forward wave and the power output is the power carried by the forward wave only. This is computed in (23).

Since (26) is a cold circuit wave it may be eliminated by properly ad-
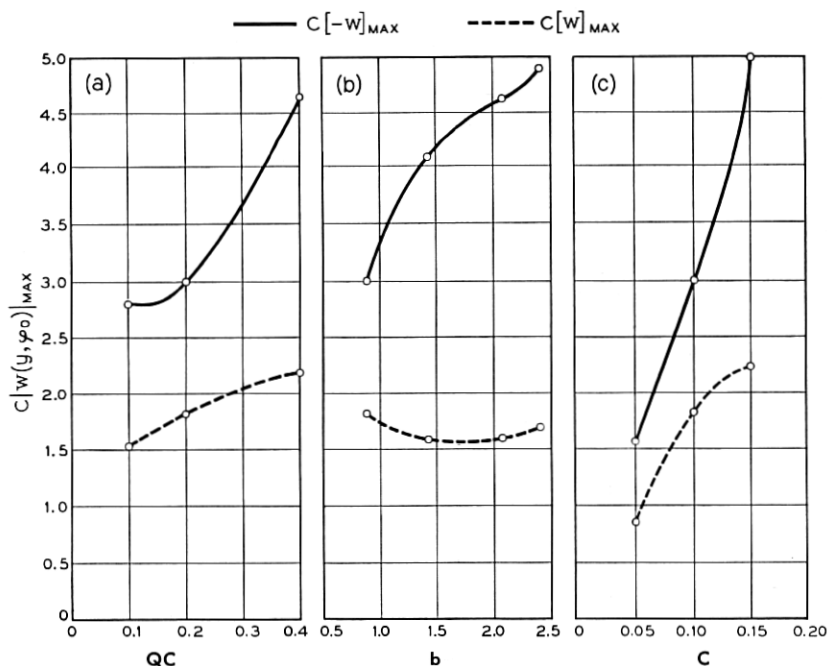
Fig. 5 — $Cw(y, \varphi_0)$ of the fast and the slowest electrons at the saturation level. (a) versus QC for $k = 2.5$, $C = 0.1$ and b for maximum small-signal gain; (b) versus b for $k = 2.50$, $C = 0.1$ and $QC = 0.2$; and (c) versus C for $k = 2.50$, $QC = 0.2$ and b for maximum small-signal gain.
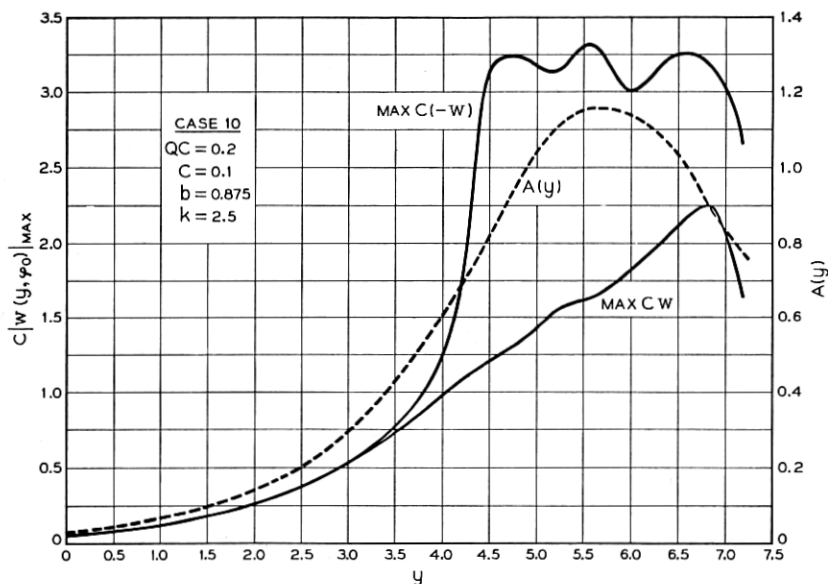
Fig. 6 — $Cw(y, \varphi_0)$ of the fast and the slowest electrons versus y for Case (10). $A(y)$ is also plotted in dotted lines for reference.

justing the impedance of the output circuit. This may be necessary in practice for the purpose of avoiding possible regenerative oscillation. In doing so, the voltage at $z = D$ is the sum of the voltage of the forward wave and that of the particular solution of the backward wave. In every case, the output power is always equal to the square of the net voltage actually at the output end divided by the impedance of the output circuit.

We find from (14), (15) and (16) that the fundamental component of electron charge density may be written as

$$\rho_\omega(z, t) = \frac{1}{2}\frac{I_0}{u_0}\left(\sin\varphi\,\frac{da_1(y)}{dy} + \cos\varphi\,\frac{da_2(y)}{dy}\right)$$

$$= \text{Real component of } \left(-\frac{1}{2}\frac{I_0}{u_0}\sqrt{\left(\frac{da_1(y)}{dy}\right)^2 + \left(\frac{da_2(y)}{dy}\right)^2}\right. \tag{26}$$

$$\left. \cdot\, e^{j\omega - \Gamma_0 z - by + j\xi}\right)$$

where $-I_0/u_0$ is the dc electron charge density, ρ_0.

If (26) is compared with (12d) or (12c), it might seem surprising that the particular solution of the backward wave is just equal to the funda-
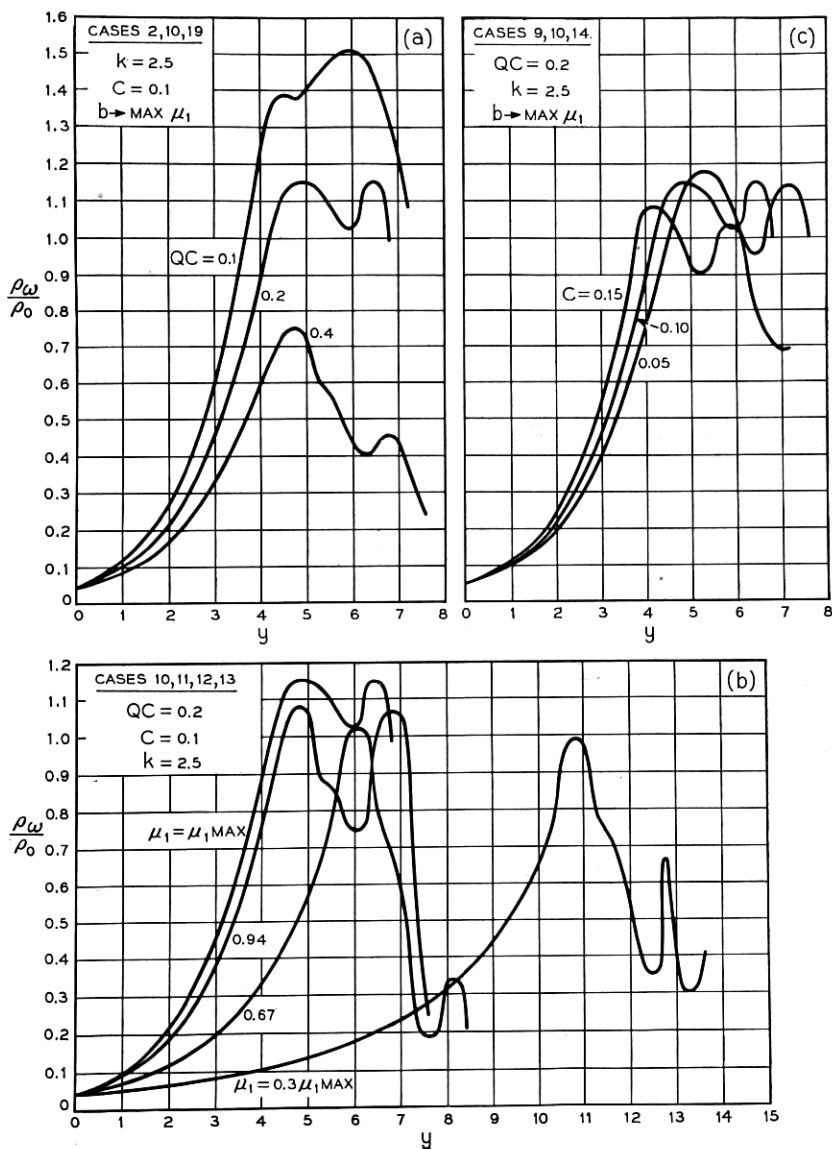
Fig. 7(a) — ρ_ω/ρ_0 versus y, (a) using QC as the parameter, for $k = 2.5$, $C = 0.1$, and b for maximum small-signal gain (Cases 2, 10, and 19); (b) using b as the parameter, for $k = 2.50$, $C = 0.1$ and $QC = 0.2$ (Cases 10, 11, 12 and 13); and (c) using C as the parameter, for $k = 2.50$, $QC = 0.2$ and b for maximum small-signal gain (Cases 9, 10 and 14).

mental component of the electron charge density of the beam multiplied by a constant

$$\left(-\frac{Z_0 I_0}{4C}\frac{C}{2(1+bC)}\frac{2u_0}{I_0}\right) \tag{27}$$

The ratio of the electron charge density to the average charge density,

$$\frac{\rho_\omega(z)}{\rho_0}$$
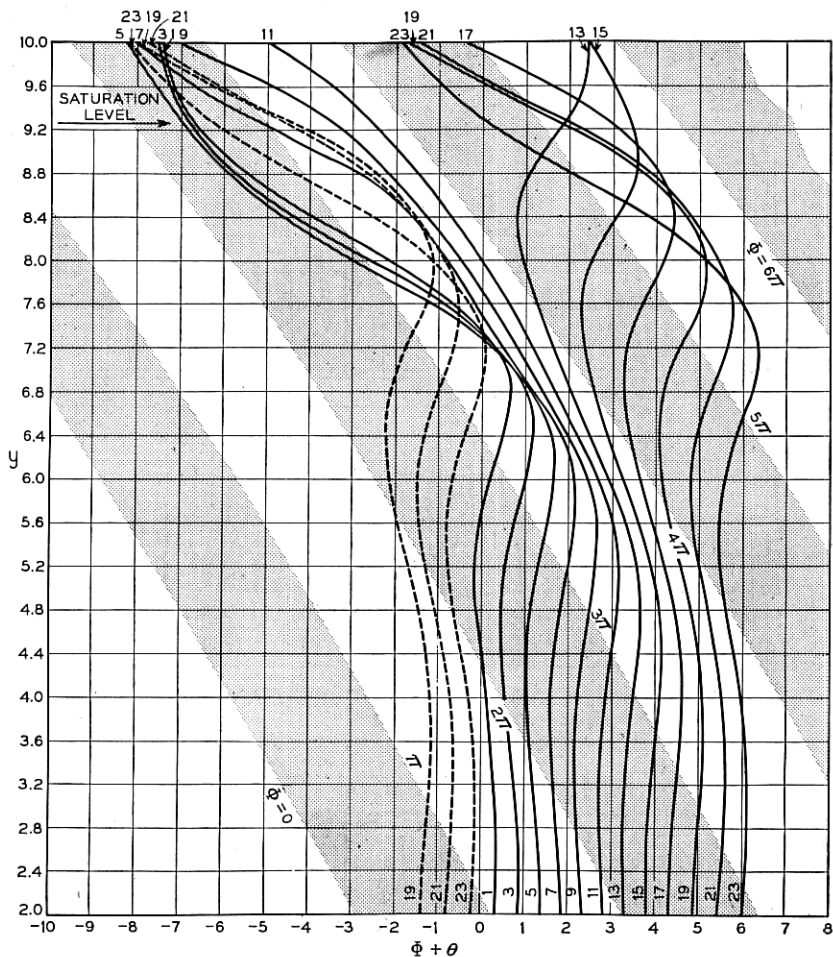
Fig. 8(a) — y versus $\varphi - by$ for $QC = 0.2$, $k = 2.5$, b for $\mu_1 = 0.67\mu_1(\max)$ and $C = $ small.

is plotted in Fig. 7 versus y, using QC, b and C, as the parameters. They are also the curves for the backward wave (the component which is coupled to the beam) when multiplied by the proportional constant given in (27). It is interesting to see that the maximum values of ρ_ω/ρ_0 are between 1.0 and 1.2 for $QC = 0.2$ and decrease as QC increases. The peaks of the curves do not occur at the saturation values of y.

10. y VERSUS $(\varphi - by)$ DIAGRAMS

To study the effect of C, b, and QC on efficiency y versus $(\varphi - by)$ diagrams are plotted in Figs. 8(b), (c), (d) and (e) for Cases (21), (16), (10) and (21), respectively. $(\varphi - by)$ here is $(\Phi + \theta)$ in Nordsieck's notation. In these diagrams, the curves numbered from 1 to 24 correspond to the 24 electrons used in the calculation with each curve for one electron. Only odd numbered electrons are presented to avoid possible confusion arisen from too many lines. The reciprocal of the slope of the curve as
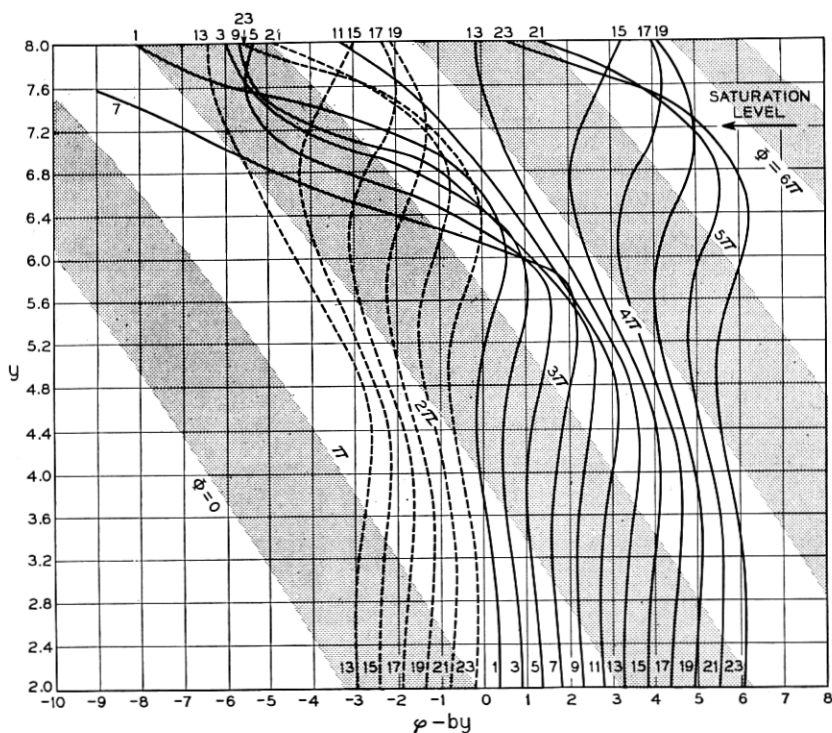

Fig. 8(b) — y versus $\varphi - by$ for $QC = 0.2$, $k = 2.5$, b for $\mu_1 = 0.67\mu_1$(max) and $C = 0.1$(Case 12).

given by (18) is proportional to the ac displacement of electron per unit of y. (In small-C theory it is proportional to the ac velocity of the electron.) Concentration of curves is obviously proportional to the charge-density distribution of the beam. In the shaded regions, the axially directed electric field of the circuit is negative and thus accelerates electrons in the positive z direction. Electrons are decelerated in the unshaded regions where the circuit field is positive. The boundaries of these regions are constant phase contours of the circuit wave. (They are constant Φ contours in Nordsieck's notation.)

These figures are actually the "space-time" diagrams which unfold the history of every electron from the input to the output ends. The effect of C can be clearly seen by comparing Figs. 8(a), (b) and (c). These diagrams are plotted for $QC = 0.2$, $k = 2.5$, b for $\mu_1 = 0.67$ $\mu_1(\max)$ and for Fig. 8(a), $C = $ small, for Fig. 8(b), $C = 0.1$, and for Fig. 8(c), $C = .15$. It may be seen that because of the velocity spread of the electrons, the saturation level in Fig. 8(a) is 9.3 whereas in Figs. 8(b) and (c), it is 7.2 and 7.0, respectively. It is therefore not surprising that Eff./C decreases as C increases.

The effects of b and QC may be observed by comparing Figs. 8(d) and (b), and Figs. 8(b) and (e), respectively. The details will not be described here. It is however suggested to study these diagrams with those given in the small-C theory.
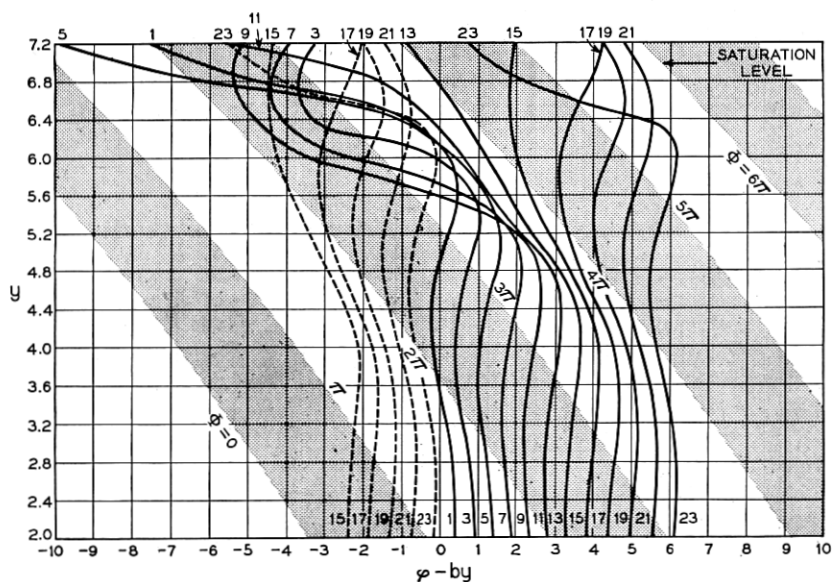

Fig. 8(c) — y versus $\varphi - by$ for $QC = 0.2$, $k = 2.5$, b for $\mu_1 = 0.67\mu_1(\max)$ and $C = 0.15$ (Case 16).

11. A QUALITATIVE PICTURE AND CONCULSIONS

We have exhibited in the previous sections the most important non-linear characteristics of the traveling wave amplifier. Numerical computations based on a model of 24 electrons have been carried out for more than twenty cases covering useful ranges of design and operating parameters. The results obtained for the saturation Eff./C may be summarized as follows:

(1) It decreases with C particularly at large values of QC.

(2) For $C = 0.1$, it varies roughly from 3.7 for $QC = 0.1$ to 2.3 for $QC = 0.4$, and only varies slightly with b.

(3) For $C = 0.15$, it varies from 2.7 to 2.5 for QC from 0.1 to 0.2 and b corresponding to the maximum small-signal gain. It varies slightly with b for $QC = 0.2$.

(4) It is almost constant between $k = 1.25$ and 2.50.

In order to understand the traveling-wave tube better, it is important to have a simplified qualitative picture of its operation. It is obvious that to obtain higher amplification, more electrons must travel in the region where the circuit field is positive, that is, in the region where electrons
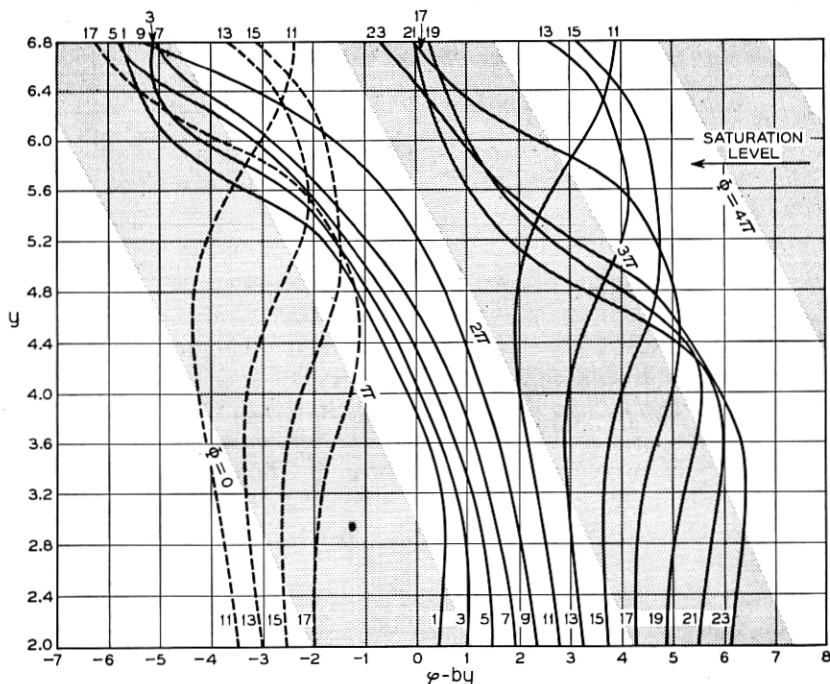

Fig. 8(d) — y versus $\varphi - by$ for $QC = 0.2$, $k = 2.5$, b for $\mu_1 = \mu_1(\max)$ and $C = 0.1$ (Case 10).
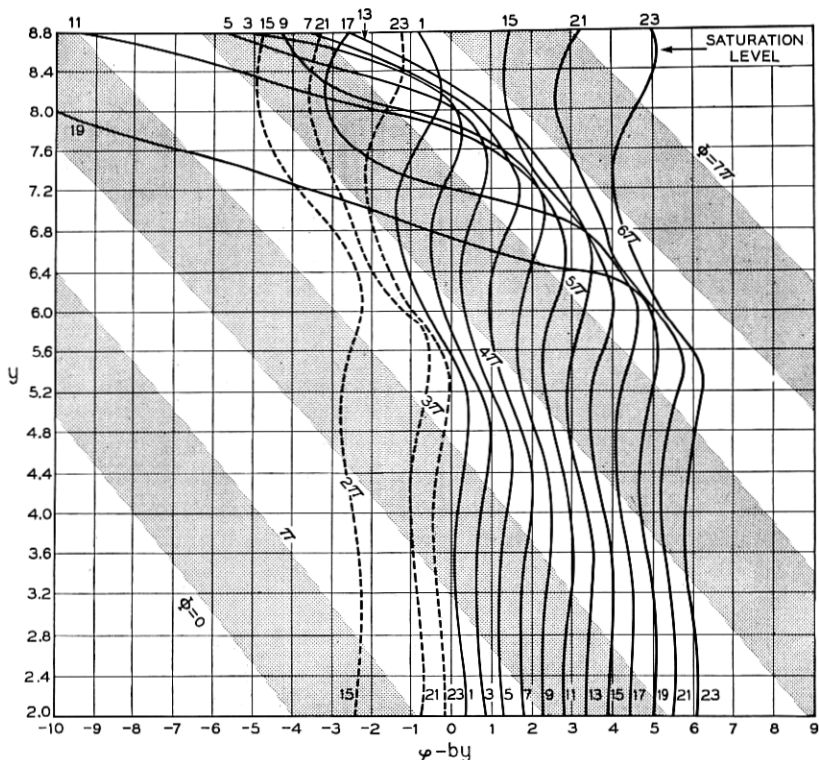
Fig. 8(e) — y versus $\varphi - by$ for $QC = 0.4$, $k = 2.5$, b for $\mu_1 = 0.67\mu_1(\text{max})$ and $C = 0.1$ (Case 21).

are decelerated by the circuit field. At the input end of the tube, electrons are uniformly distributed both in the accelerating and decelerating field regions. Bunching takes place when the accelerated electrons push forward and the decelerated ones press backward. The center of a bunch of electrons is located well inside the decelerating field region because the circuit wave travels slower than the electrons on the average (b is positive). The effectiveness of the amplification, or more specifically the saturation efficiency, therefore depends on (1), how tight the bunching is, and (2), how long a bunch travels inside the decelerating field region before its center crosses the boundary between the accelerating and decelerating fields.

For small-C, the ac velocities of the electrons are small compared with the dc velocity. The electron bunch stays longer with the decelerating circuit field before reaching the saturation level when b or QC is larger. On the other hand, the space charge force, or large QC or k tends to distort the bunching. As the consequence, the saturation efficiency increases with b, and decreases as k or QC increases. When C becomes finite how-

ever, the ac velocities of the electrons are no longer small as compared with their average speed. The velocity spread of the electrons becomes an important factor in determining the efficiency. Its effect is to loosen the bunching, and consequently it lowers the saturation level and reduces the limiting efficiency. It is seen from Figs. 5 and 6 that the velocity spread increases sharply with C and also steadily with b and QC. This explains the fact that in the present calculation the saturation Eff./C decreases with C and is almost constant with b whereas in the small-C theory it is constant with C and increases steadily with b.

12. ACKNOWLEDGEMENTS

APPENDIX

The initial conditions at $y = 0$ are computed from Pierce's linearized theory. For small-signal, we have

$$a_1(y) = 4A(y) \cos (b + \mu_2)y \tag{A-1}$$

$$a_2(y) = -4A(y) \sin (b + \mu_2)y \tag{A-2}$$

$$A(y) = \epsilon e^{\mu_1 y} \tag{A-3}$$

Here ϵ is taken equal to 0.03, a value which has been used in Tien-Walker-Wolontis' paper. Define

$$\frac{\partial X}{\partial y} = w(y, \varphi_0) \qquad \text{(A-4)} \qquad\qquad X = pe^{-j\varphi_0} + p^* e^{j\varphi_0} \qquad \text{(A-5)}$$

where p^* is the conjugate of p. After substituting (A-1) to (A-5) into the working equations (15) to (18) and carrying out considerable algebraic work, we obtain exactly Pierce's equation.[16]

$$\mu^2 = \frac{(1 + jC\mu)(1 + bC)}{(j - \tfrac{1}{2}C\mu + j\tfrac{1}{2}bC)(\mu + jb)} - 4QC(1 + jC\mu)^2 \tag{A-6}$$

provided that

$$-\left(\frac{\omega_p}{\omega C}\right)^2 \int_{-0}^{+\infty} e^{-k|\varphi(y,\varphi_0+\phi)-\varphi(y,\varphi_0)|[1+ Cw(y,\varphi_0+\phi)]}$$

$$\cdot \, d\phi \, \text{sgn} \, (\varphi(y, \varphi_0 + \phi) - \varphi(y, \varphi_0)) = 8\epsilon QC \tag{A-7}$$

$$\cdot \, |(1 + jC\mu)(\mu + jb)| \, e^{\mu_1 y} \cos (\arg [(1 + jC\mu)(\mu + jb)] + \mu_2 y - \varphi_0)$$

Here $\mu = \mu_1 + j\mu_2$ or Pierce's $x_1 + jy_1$. From (A-7) the value of ω_p is determined for a given QC. The ac velocities of the electrons are derived from (A-4), such as,

$$w(y, \varphi_0)$$
$$= -2\epsilon \left| \mu \frac{\mu + jb}{1 + jc\mu} \right| e^{\mu_1 y} \cos\left(\arg\left[\mu\left(\frac{\mu + jb}{1 + jC\mu}\right)\right] + \mu_2 y - \varphi_0 \right) \quad \text{(A-8)}$$

(A-1), (A-2), (A-7) and (A-8) are the expressions used to calculate the initial conditions at $y = 0$, when μ_1 and μ_2 are solved from Pierce's equation (A-6).

From (12c), the particular solution of the backward wave at small-signal is found to be

$$B(z, t) = -2\epsilon \left| \frac{-2jC(1 + jC\mu)(\mu + jb)}{2j - c\mu + icb} \right| e^{\mu_1 y}$$
$$\cos\left[\arg\left[\frac{-2jC(1 + jC\mu)(\mu + jb)}{2j - C\mu + jcb} \right] + \mu_2 y - \varphi_0 \right]$$

which agrees with Pierce's analysis.[17]

REFERENCES

1. J. R. Pierce, Traveling-Wave Tubes, D. Van Nostrand Co., N.Y., 1950, p. 160.
2. R. L. Hess, Some Results in the Large-Signal Analysis of Traveling-Wave Tubes, Technical Report Series No. 60, Issue No. 131, Electronic Research Laboratory, University of California, Berkeley, California.
3. C. K. Birdsall, unpublished work.
4. J. J. Caldwell, unpublished work.
5. P. Parzen, Nonlinear Effects in Traveling-Wave Amplifiers, TR/AF-4, Radiation Laboratory, The Johns Hopkins University, April 27, 1954.
6. A. Kiel and P. Parzen, Non-linear Wave Propagation in Traveling-Wave Amplifiers, TR/AF-13, Radiation Laboratory, The Johns Hopkins University, March, 1955.
7. A. Nordsieck, Theory of the Large-Signal Behavior of Traveling-Wave Amplifiers, Proc. I.R.E., **41**, pp. 630–637, May, 1953.
8. H. C. Poulter, Large Signal Theory of the Traveling-Wave Tube, Tech. Report No. 73, Electronics Research Laboratory, Stanford University, California, Jan., 1954.
9. P. K. Tien, L. R. Walker and V. M. Wolontis, A Large Signal Theory of Traveling-Wave Amplifiers, Proc. I.R.E., **43**, pp. 260–277 March, 1955.
10. J. E. Rowe, A Large Signal Analysis of the Traveling-Wave Amplifier, Tech. Report No. 19, Electron Tube Laboratory, University of Michigan, Ann Arbor, April, 1955.
11. P. K. Tien and L. R. Walker, Correspondence Section, Proc. I.R.E., **43**, p. 1007, Aug., 1955.
12. Nordsieck, op. cit., equation (1).
13. L. Brillouin, The Traveling-Wave Tube (Discussion of Waves for Large Amplitudes), J. Appl. Phys., **20**, p. 1197, Dec., 1949.
14. Pierce, op. cit., p. 9.
15. Nordsieck, op. cit., equation (4).
16. Pierce, op. cit., equation (7.13).
17. J. R. Pierce, Theory of Traveling-Wave Tube, Appendix A, Proc. I.R.E. **35**, p. 121, Feb., 1947.